LA-UR-21-21769
Approved for public release; distribution is unlimited.

Title: xRage simulations of magnetic velocity gauges used in gas gun shock initiation experiments

Author(s): Menikoff, Ralph

Intended for: Report

Issued: 2021-02-23

xRage simulations of magnetic velocity gauges used in gas gun shock initiation experiments

Ralph Menikoff

February 17, 2021

1 Introduction

Shock initiation gas gun experiments of PBX 9012 have been performed by Burns and Chiquete [2020] using magnetic velocity gauges as the principal diagnostic. In private communications, the experimenters noted that compatibility issues required a different glue to bond the gauges to PBX 9012 then previously used for experiments with PBX 9501 and PBX 9502. The silicon glue used is more viscous and can result in glue layers up to 50 microns, which is about the gauge thickness. This raises the question on what affect the thicker glue layers have on the gauge response. In particular, the width of the lead shock can affect the accuracy of inferring shock locus points used for the shock pressure of Pop plot data points and for Hugoniot data to calibrate the reactants EOS.

The particle velocity of the initial shock is determined by a stirrup gauge on the front surface of the HE. In principle, the gauge response can be determined from 1-D simulations that resolves the gauge layers (25 μm teflon + 5 μm Al + 25 μm teflon) plus the glue bonding the gauge to the HE, when the gauge is impacted by a projectile. The change in the magnetic flux, which determines the gauge velocity, is proportional to the integral of the velocity along the active element of the gauge. For perfect alignment between the projectile and HE, the active gauge element is in the plane of the shock front and its velocity is uniform across the active element. The gauge velocity time history would then correspond to the velocity of a Lagrangian tracer particle in the Al.

Physically one expects the flow to consist of a sharp lead shock followed by wave interactions and their reflections at the interfaces between materials. Since the gauge is thin, after a short time the particle velocity of all the layers will equilibrate to the value from the impedance match of the projectile directly on the reactants HE. A misalignment or tilt between the projectile and the HE would cause a time shift of the velocity time histories along points on the active gauge element. This would smear out the rise time of the lead shock in the gauge time history. Consequently, the response of a stirrup gauge is characterized by two quantities; the gauge rise time of the lead shock and the equilibration time to the impedance match velocity. We show

that the tilt can be accounted for with a running average over the 1-D simulated gauge time history.

The gauge shock rise time can depend on tilt from either misalignment or a variation in glue thickness along the active gauge element. The equilibration time depends on the thickness of the gauge layers and increases with the thickness of the glue layer. Also these times are expected to decrease with projectile velocity since the lead shock pressure and hence the wave speeds in the gauge materials would increase.

Stirrup gauge velocity time histories for all 5 experiments are shown in fig. 1. The rise times of the lead shock are up to 30 ns and the equilibration time up to 100 ns. Two shots 1s1674 and 2s1101 have an anomalous toe before the lead shock. In all cases, the plots show there is negligible reaction in the first 150 ns. This is important for accurately determining the particle velocity behind the lead shock.

Another indication of tilt is the time difference between the tracker gauges seen in fig. 2; $\Delta t = \ell\theta/u_s$ where ℓ is the distance between trackers, about 20 mm for the left and right tracker gauges, θ is tilt angle in radians and u_s is the shock speed. The time difference should decrease for the downstream trackers since the shock speed increases with distance of run. As shown next, the tilt angle for lead shock is larger than the impact tilt angle determined from the shock rise time of the stirrup gauge.

As noted by Gustavsen et al. [2012, §III.B], the impact tilt angle and the shock tilt angle are related by Snell's law. For small angles, this reduces to $\theta_{shock} = (u_{shock}/u_{projectile}) \cdot \theta_{impact}$. Moreover, for small angles, to leading order in θ, the shock speed is determined by the planar shock impedance match. For the largest pressure shots, 1s1673 and 2s1101, $u_{shock}/u_{projectile}$ are 5.4 and 2.7, respectively. The large difference is due to the projectile EOS; sapphire for single-stage gas gun shots and KelF for the two-stage gas gun shot.

As illustrative examples of the magnitude of the time difference between the left and right trackers: For shot 1s1673 with $\theta_{impact} = 1$ milliradian and $u_s = 5$ km/s, Δt would be 22 ns. For shot 2s1101 with $\theta_{impact} = 5$ milliradian and $u_s = 5$ km/s, the would be 54 ns.

Figure 2 shows for shot 2s1101 that the time difference between tracker gauges are neither constant nor monotonically, and for shot 1s1675 and 1s1673 the time difference is up to 50 ns. This can be explained by a different glue thickness under each gauge. Another anomaly is that the shock arrival time for the velocity gauges are not always between the time of the left and right tracker gauges, which is expected since the active element of the velocity gauge is between that of the left and right tracker gauges; see [Burns and Chiquete, 2020, fig 1]. If the shock arrival time was chosen to correspond to first motion of the velocity gauge, then a bowing in the glue thickness under the active gauge element could explain the anomaly.

In contrast to the stirrup gauge, the embedded velocity gauges are oblique to the plane of the shock front. Consequently, 2-D simulations are needed to determine the response of the gauge. Moreover, oblique shock interactions lead to shear layers, that is, tangential velocity discontinuity along the interfaces between the HE and the gauge. Bdzil [2018] has raised the issue of whether the slip layers cause the gauge velocity to differ from the HE particle particle

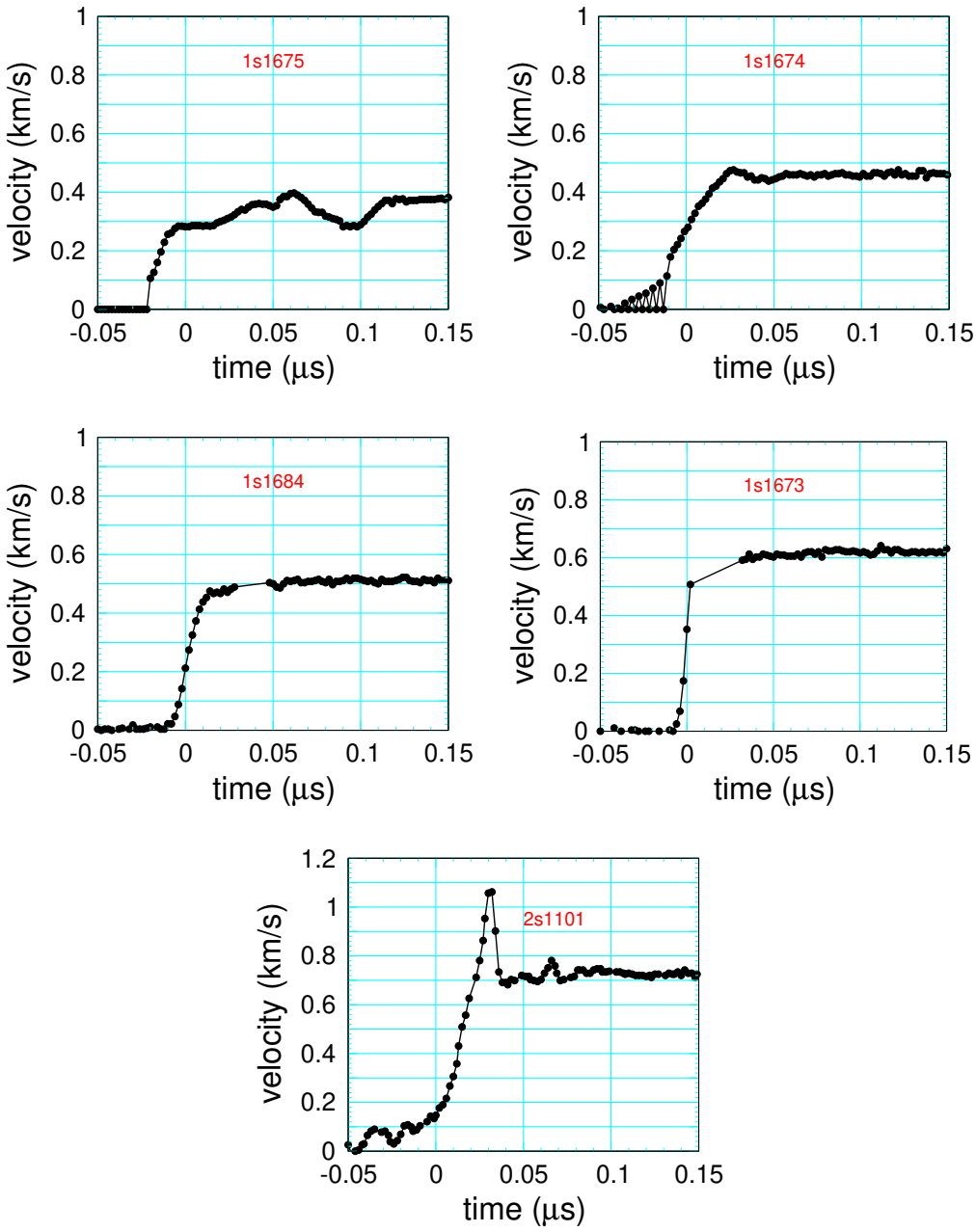

Figure 1: Stirrup gauge velocity time histories for PBX 9012 experiments of Burns and Chiquete [2020]. The straight line segments for shots 1s1684 and 1s1673 are from missing data points. Plots of gauge time histories for each experiment in pdf files the experimentalist put on the smallscale database shows for 1s1673 the lead shock overshoots the final velocity and then decreases below the final velocity, and for 1s1684 there is an overshoot before reaching the final velocity.

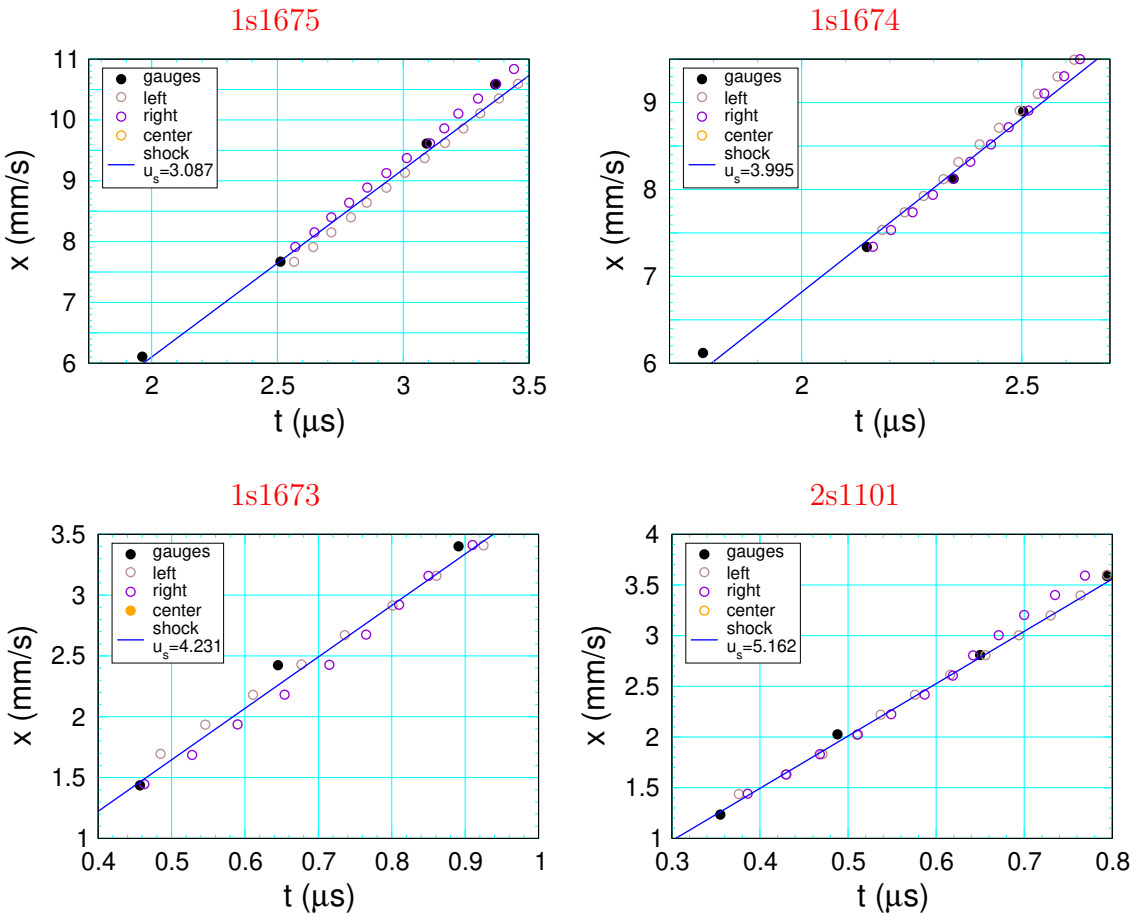

Figure 2: Tracker data at early time (before transition to detonation) for PBX 9012 experiments of Burns and Chiquete [2020]. Data for shot 1s1684 is not shown since left and right tracker did not report. Blue line is linear fit only meant to get an estimate of shock speed needed to determine change in glue thickness that would be needed to explain time difference between gauges at the same position.

velocity, and hence a systematic error with associating the gauge velocity with the HE particle velocity. The simulations for PBX 9012 shown in later section do show this effect with the velocities differing by about 3 percent for a 6 GPa shock.

The embedded velocity gauge time histories are shown in fig. 3. The plots show that the shock rise time of the early velocity gauges varies within an experiment and is up to 80 ns. As with the tracker gauges the time variation can be explained by different glue layer thickness under each gauge.

A large gauge shock rise time can affect the interpretation of the gauge time history when reaction causes the velocity to increase following the lead shock. For example, the gauge at 3.59 mm of shot 2s1101: Is the lead shock particle velocity at 2.0 km/s followed by an increase to a peak at 2.3 or is shock particle velocity at the peak followed by a decreasing velocity ?

We also note that the gauge equilibration time decreases with the lead shock strength due to the increase in shock speed. In addition, the length of the active gauge element decreases

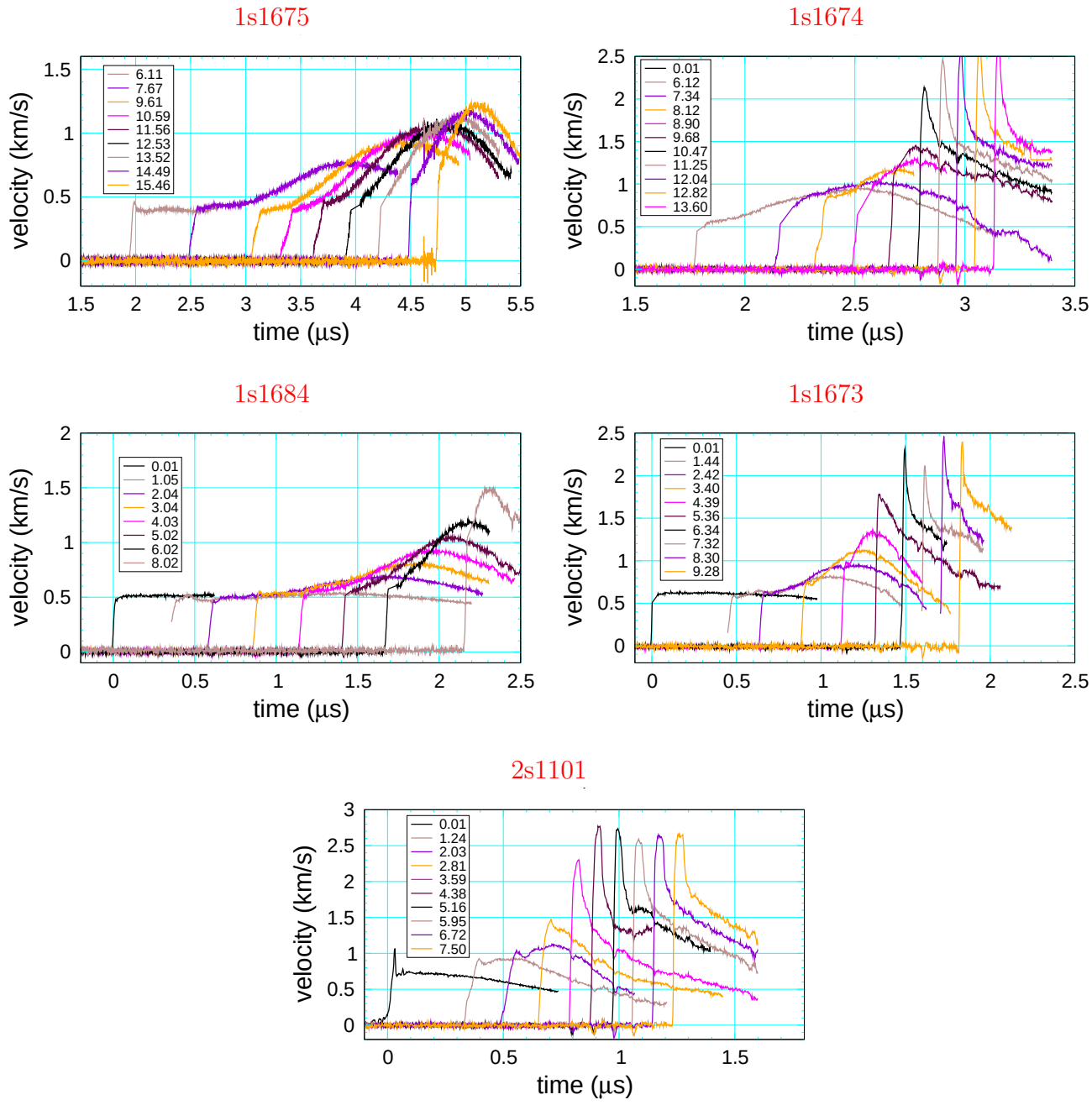

Figure 3: Velocity gauge time histories for PBX 9012 experiments of Burns and Chiquete [2020].

with distance of run and hence the gauge rise time decreases. Consequently, if a transition to a detonation occurs, both effects cause the gauge rise time for a detonation wave to be sharper than the shock rise time before detonation. This is seen in the velocity gauge plots.

The following sections show results of xRage simulations on the response time of the stirrup and oblique gauges using conditions corresponding to those in some of the PBX 9012 experiments.

2 Gauge geometry

With perfect alignment, the shock direction, the direction of the active element of the gauge (the conductor at the end of the loop, see [Burns and Chiquete, 2020, fig 1]) and the magnetic field direction are mutually orthogonal. The velocity gauge responds to the change in the magnetic flux, which is proportional to the integral along the active gauge element of the velocity component in the shock direction.

Furthermore, for the stirrup gauge the layers of the gauge package (25 μm teflon / 5 μm Al / 25 μm teflon) are normal to the shock direction, that is, the leads of the conductor are in the plane of the shock front. Consequently, the shock impacts the active gauge element simultaneous along its length. The fluid flow is one-dimensional in the direction of shock propagation and the gauge velocity is proportional to the velocity of the Al conductor.

With a small misalignment or tilt angle between the normal to the gauge layers and shock propagation direction, Lagrangian time histories along points on the active gauge element are shifted linearly in time. To a good approximation the gauge velocity is a running time average over the Lagrangian time history of the Al in a 1-D simulation, that is, tilt smears out the lead shock rise time of the gauge velocity.

For the embedded velocity gauges, the angle between the normal to the gauge layers and the shock propagation direction is non-zero, nominally 30 degrees. Consequently, even with perfect alignment the flow is 2-dimensional in plane of the shock direction and the magnetic field direction. The oblique impact of the shock with the gauge package leads to 2-D wave patterns that can be analyzed with shock polars rather than the simple 1-D shock impedance matches that occur with the stirrup gauge; see [Bdzil, 2018] and [Romick et al., 2020]. Again misalignment would smear out the lead shock rise time of the velocity gauge, and can be accounted for with a running time average of the simulated Lagrangian time history of point corresponding to active gauge element.

3 1-D stirrup gauge simulations

For the PBX 9012 experiments, Burns (in e-mail) said that he measured the glue layer thickness surrounding the stirrup gauge. The thicknesses were about 50 μm for shots 2s1101 and 1s1673. However, the glue thickness under the gauge package may vary and be different under the active gauge element. To see the effect of a thick glue layer simulations of the stirrup gauge were run for these 2 shots with a nominal glue thickness of 25 μm.

We note that for a shock rise time Δt, the tilt angle is $\theta = u_{proj}\Delta t/w$ where u_{proj} is the projectile velocity and $w = 10\,\text{mm}$ is the length of the active element of the stirrup gauge.

3.1 Shot 2s1101

Shot 2s1101 had a KelF projectile with velocity of 1.555 km/s. Simulated and experimental stirrup gauge data are shown in fig. 4. Several points to note:

1. In the simulated data time history, the first plateau (0.8 km/s) corresponds to the impedance match into the teflon, the second plateau (1.0 km/s) to the impedance match into the glue, and the final velocity to the impedance match of the projectile directly into the 9012 reactants.
2. The arrival time of the lead shock at the gauge is ahead of the lead shock at the HE interface by about 16 ns. This would increase with glue thickness.
3. The final velocity of the simulation is slightly higher than the average velocity of the gauge. This may be due to either the EOS models used in the simulation or the accuracy of the gauge velocity.
4. The experimental shock rise time of 30 ns corresponds to a tilt angle between the projectile and stirrup gauge of 4.6 milliradians.
5. The experimental gauge time history has a low amplitude toe over 40 ns. It is not clear what would cause the toe.
6. Neglecting the toe, the final velocity at the gauge is achieved after about 55 ns from the arrival of the lead shock. Again, this would increase with glue thickness.
7. The smoothed simulated gauge data is qualitative but the peak is low and the time to equilibrating the final velocity is a little large.

Figure 5 shows simulated gauge time history for a 50 μm glue thickness. Compared to 25 μm glue thickness, there are two significant differences. First, the time to equilibrate to the final

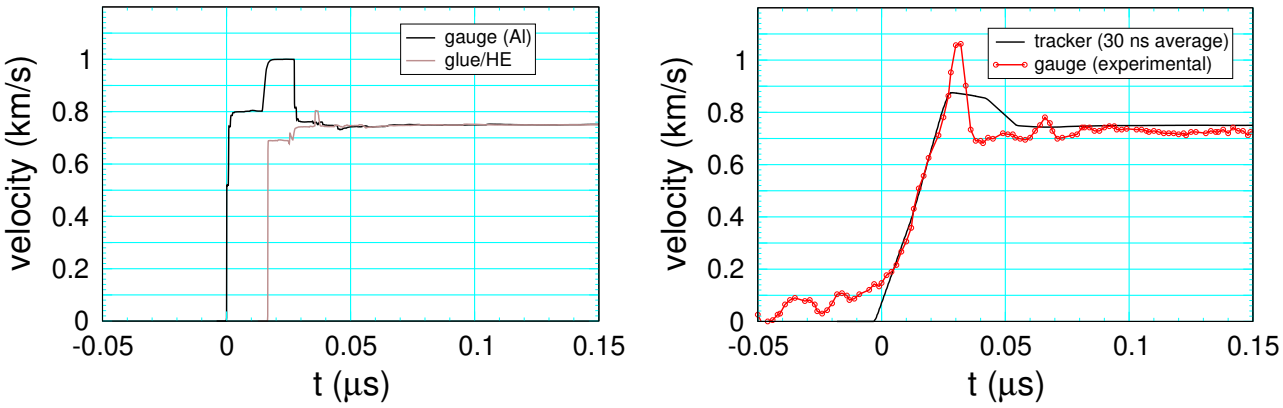

Figure 4: Stirrup gauge velocity time histories for shot 2s1101 from 1-D simulation with glue thickness of 25 μm and experimental data.

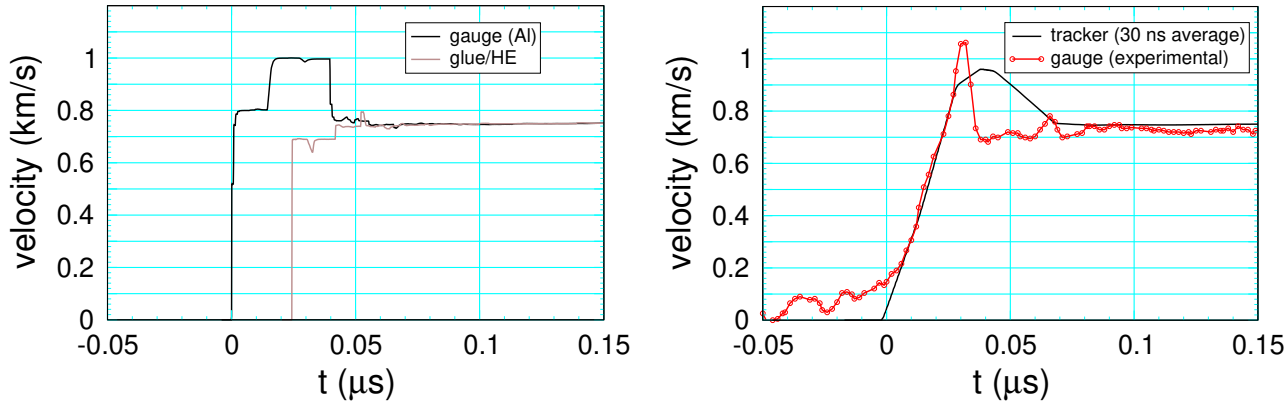

Figure 5: Stirrup gauge velocity time histories for shot 2s1101 from 1-D simulation with glue thickness of 50 μm and experimental data.

velocity has increased from 55 to 68 ns. Second the time difference between the arrival of the lead shock at the stirrup gauge and at the HE interface has increased from 16 to 25 ns. Since the time origin for the embedded gauge data is intended to be the arrival of the shock at the HE interface, the glue thickness of the stirrup gauge affects the time origin.

3.2 Shot 1s1684

Shot 1s1684 had a sapphire projectile with velocity of 0.605 km/s. Simulated and experimental stirrup gauge data are shown in fig. 6. Compared to fig. 4, there are stronger reflected waves off the projectile due to sapphire having a much stiffer EOS than KelF.

The lead shock rise time of the experimental gauge is 20 ns. This would correspond to an impact tilt angle of 1.2 milliradians. Alternatively, the same tilt angle can be obtained by varying the glue layer thickness along the length of the active gauge element by 12 μm.

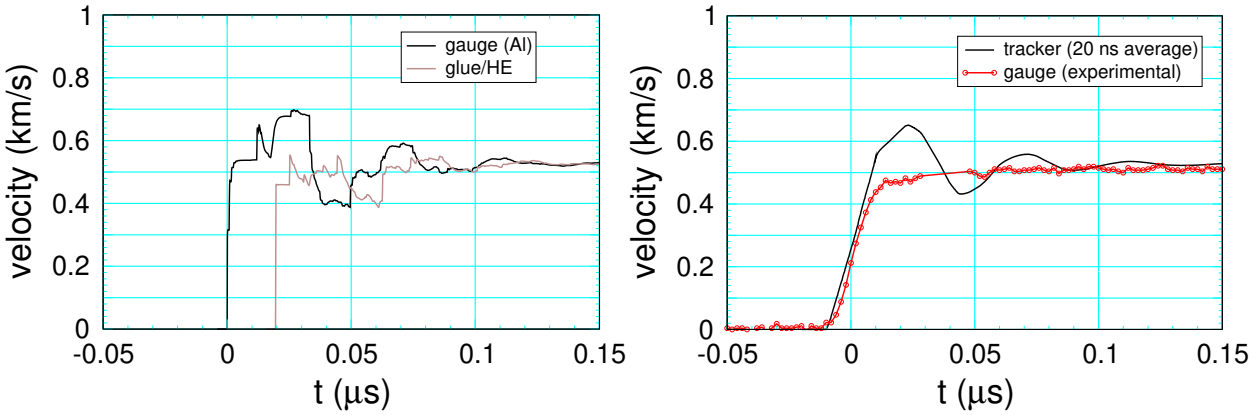

Figure 6: Stirrup gauge velocity time histories for shot 1s1684 from 1-D simulation with glue thickness of 25 μm and experimental data.

As noted in the caption to fig. 1, there are some missing data points in the plot of the experimental stirrup gauge (red curve). With the points shown in velocity gauge plot on the smallscale database for shot 1s1684, the time to equilibrate to the final velocity would be close to 50 ns. Even with this correction the simulated gauge equilibrium time is too large. This suggest the glue thickness below the active gauge element was less than 25 μm.

4 2-D stirrup gauge simulation

Two-D simulations of the stirrup gauge can account for variations in the thicknesses of the gauge and glue layers. Figure 7 shows the initial setup for shot 1s1684. The shock propagates in the y-direction, the active gauge element is in the x-direction, and the magnetic field is directed into the plane of the figure. The red region is the projectile and the green region is the PBX 9012 reactants. The glue layer is the blue region. Its thickness is tapered from 25 μm on left the to 19 μm on the right over a width of 5.2 mm. The light green is 50 μm thick teflon layer representing the gauge package. This leaves a wedge of air between the teflon and the projectile varying in thickness from 0 μm on the left to 6 μ on the right. The conductors connecting the active gauge element run in to the plane of the figure.

The aluminum gauge layer was left out since the thin layer would require very fine resolution and add little to the point of this simulation. Tracer particles in the middle of the teflon 1 mm apart were used to get the y-component of the velocity time histories along points on the active gauge element. The gauge velocity corresponds to the integral of the velocity over the active gauge element. This can be approximated as the average velocity of the tracers.

The tracer time histories are shown in fig. 8. Since the angle of the air layer is very small (1.2 milliradians), the motion in the horizontal direction is very small. Effectively, the tracer time histories are the same as time shifted 1-D time histories for the glue thickness over the tracer point. Moreover with the small change in glue thickness, there is little difference (other then the time shift) between the tracer time histories. This is the justification for the running time average of the time histories for the 1-D simulation to account for tilt.

Figure 7: Density plot of initial configuration for 2-D simulation of stirrup gauge.

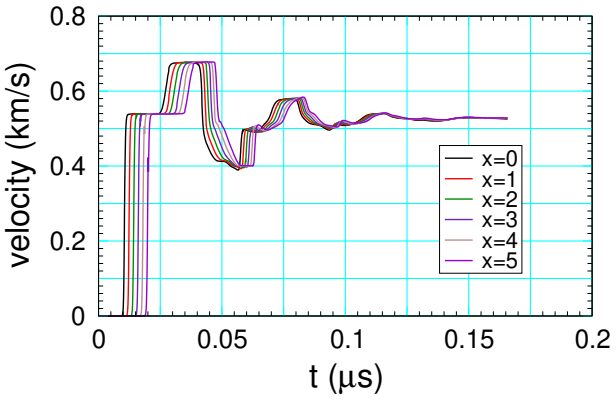

Figure 8: Velocity time histories for tracer particles along active element of the stirrup gauge.

5 2-D oblique velocity gauge simulations

Two-D simulations are needed to model the effect of the glue layers next to the gauge package for the embedded oblique velocity gauges. Figure 9 show the initial setup. The shock propagates in the y-direction, the magnetic field is in the x-direction, and the active element of the gauge is directed into the plane of the figure. Blue regions on the sides are air. Bright orange inflow region at the bottom is given the state of a 6 GPa reactants shock and drives the flow. Yellow regions are PBX 9012 reactants. The oblique gauge package consists of the dull orange 50 micron layer of teflon surrounded on each side by the turquoise 25 micron glue layers of sylgard. The mesh is $-2.5 < x < 2.5$ mm and $-0.1 < y < 2.55$ mm. The conductors connecting to the active gauge element run up to the left and parallel to the oblique gauge layers shown in the figure. For comparison, a second simulation was run without the glue layers.

The gauge velocity corresponds to the y-component of the particle velocity at the center of teflon layer. If the active element Al conductor were included in the simulation, it would be a

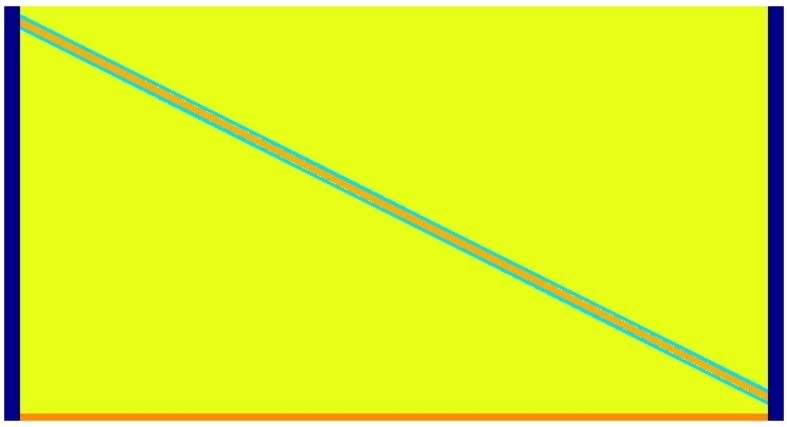

Figure 9: Density plot of initial configuration for a 2-D simulation of the oblique velocity gauge at 30 degree angle.

rectangular region 1 mm wide and 5 microns thick embedded in the center of the oblique teflon layer at $x = 0$.

Figures 10 and 11 show zoomed in plots about wave interactions along center line $x = 0$ with and without the glue layer. The mesh for these plots are $-0.15 < x < 0.85$ mm and $0.4 < y < 1.4$ mm. The color scale (blue to red) is 0 to 3 g/cc for the density, 0 to 8 GPa for the pressure and 0 to 1 km/s for the y-component of the velocity. The horizontal width of the gauge in the density plot sets the spatial scale; 0.2 mm with glue and 0.1 mm without glue.

Since there is no reaction in the simulations, after the wave interactions, the shock front in the HE is behind but parallel to the incident shock front and with the same shock state as before the interaction. This is the analogue of the stirrup gauge equilibrating to the velocity of the impedance match for the projectile directly impacting the HE.

The interaction width transverse to the front increases substantially with the 25 thick glue layers. In addition, the perturbation in the pressure is significantly larger with the glue. This

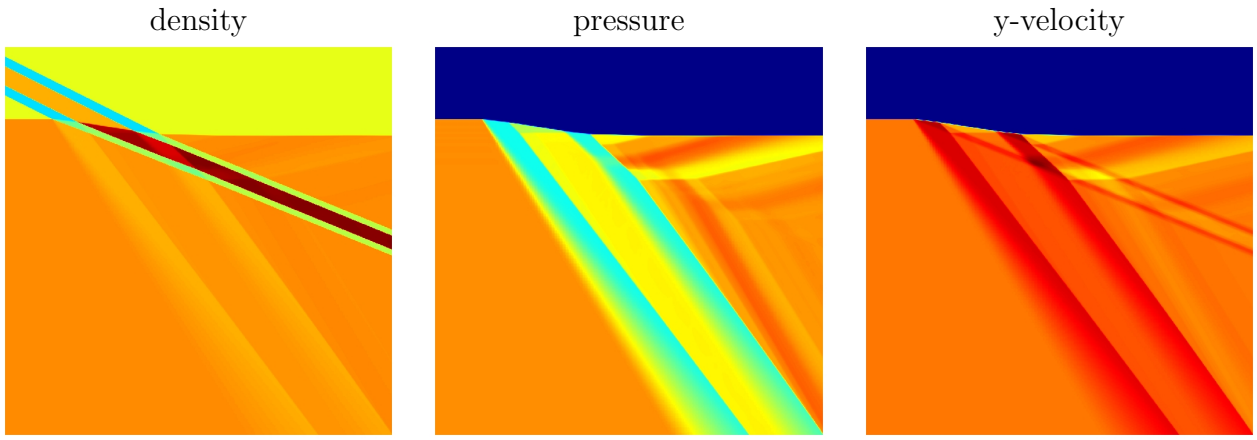

Figure 10: Shock interaction for oblique gauge and 25 micron thick glue layer both upstream and downstream of the gauge.

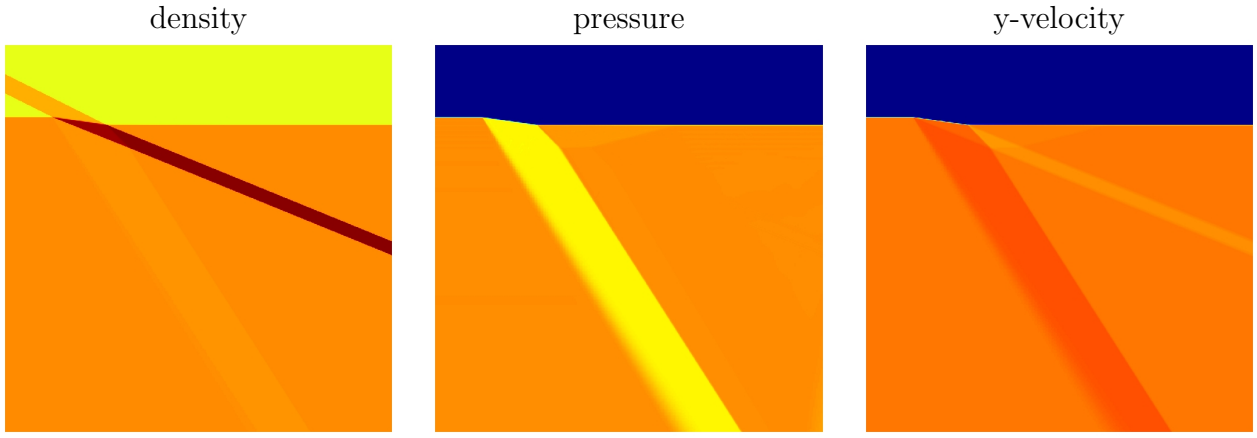

Figure 11: Shock interaction for oblique gauge without glue layers.

is important for a shock-to-detonation transition as the change in thermodynamic state on the downstream side of the gauge would affect the reaction (not included in the simulations) in the HE; that is, the benefit of the teflon being good impedance match to the HE is greatly reduced.

The shear layers noted by Bdzil [2018] are clearly seen in the velocity plot. They are on both the upstream and downstream side of the gauge and the glue layers. The discontinuity in velocity is larger with the glue. This is likely due to the softer EOS of the glue as compared to the EOS of the teflon and the reactants.

Time histories of the pressure and y-velocity for the gauge (middle of teflon) and both the upstream and downstream HE interfaces are shown in 12 and 13. There are significantly larger perturbations with the glue. It also takes longer to equilibrate the y-velocity. Moreover, after the interactions, the y-velocity of the gauge is lower than the reactants by 3.4 % and 3.2 %

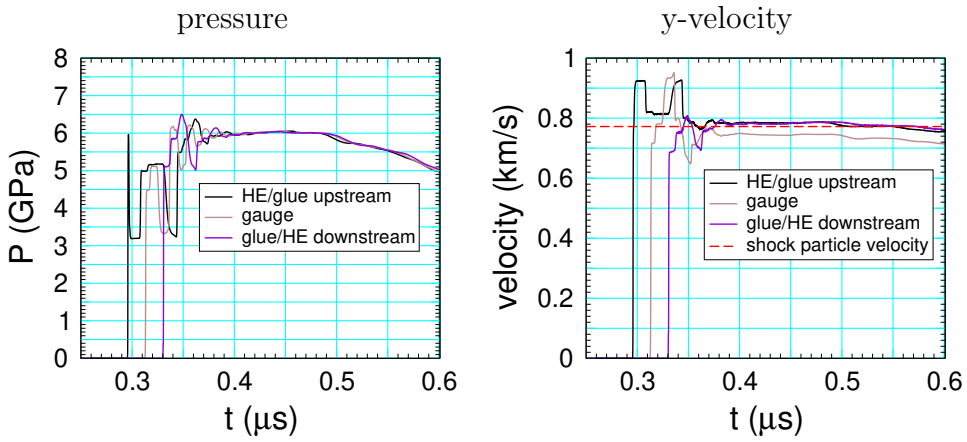

Figure 12: Lagrangian tracer plots for 6 GPa shock impacting oblique gauge with 25 μm glue layers. Tracers initially alone center line of initial density figure. Gauge velocity corresponds to tracer at center of teflon.

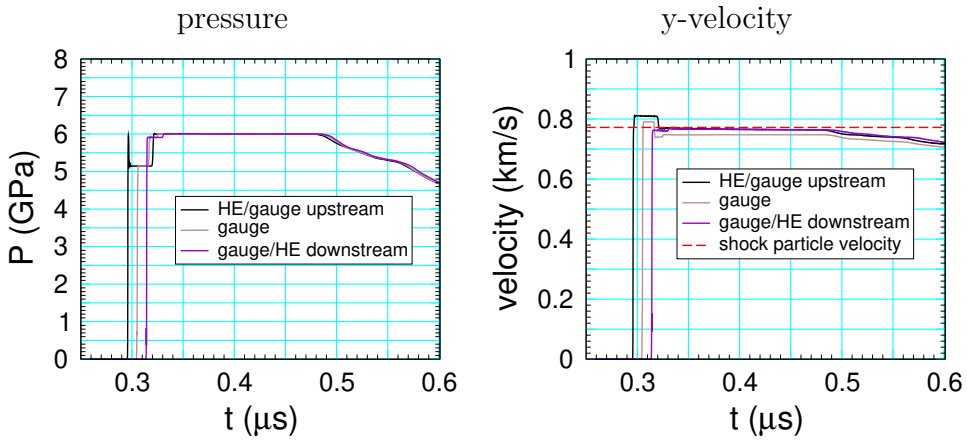

Figure 13: Lagrangian tracer plots for 6 GPa shock impacting oblique gauge without glue layers. Tracers initially alone center line of initial density figure. Gauge velocity corresponds to tracer at center of teflon.

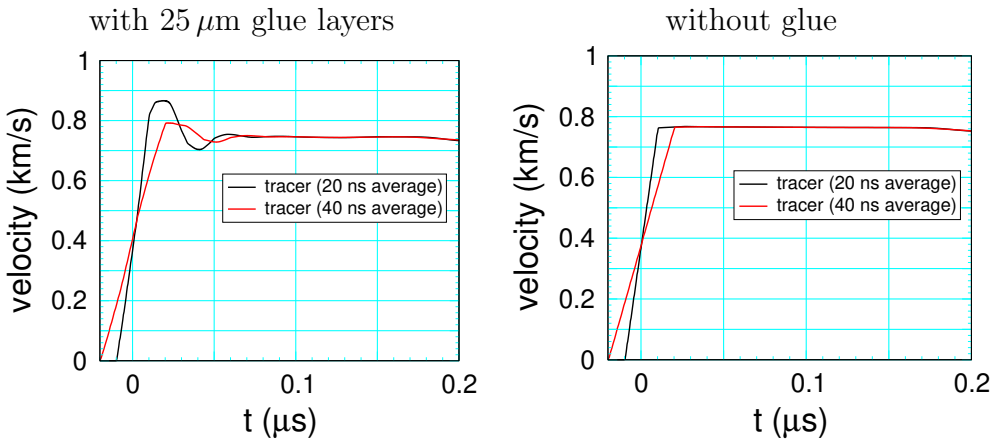

Figure 14: Running average simulated gauge velocity with and without glue layers.

with and without the glue, respectively. Thus, there is a systematic error in the gauge velocity. Overall the thick glue layer degrades the response of the velocity gauge. With HE reaction, the gauge response time can affect identifying where the lead shock profile ends and the velocity increase from reaction begins, leading to increased uncertainty in the shock particle velocity.

The falloff of the pressure at $t = 0.5\,\mu$s is due to side rarefactions since the HE in the simulation is only 5 mm wide, which is much smaller than the HE width in the experiments (75 mm and 50 mm for single-stage and two-stage gas guns, respectively.)

The effect on the simulated shock rise time due to tilt is shown in fig. 14. With a 25 μm glue layer there is a small oscillation in the time history after the shock rise similar to that for the simulated stirrup gauges, and some of the early experimental velocity gauges; for example, in shot 2s1101 shown in fig. 3.

References

J. B. Bdzil. Fluid Mechanics of an Obliquely Mounted MIV Gauge. Technical report, Los Alamos National Lab., March 2018. LA-UR-18-22397.

M. J. Burns and C. Chiquete. Shock initiation of the HMX-based explosive PBX 9012: Experiments, uncertainty analysis, and unreacted equation-of-state. *J. Appl. Phys.*, 127:215107, 2020. URL https://doi.org/10.1063/1.5144686.

R. L. Gustavsen, R. J. Gehr, S. M. Bucholtz, R. R. Alcon, and B. D. Bartram. Shock initiation of triaminotrinitrobenzene base explosive PBX 9502 cooled to -55 C. *J. Appl. Phys.*, 112, 2012. URL http://dx.doi.org/10.1063/1.4757599.

C. M. Romick, T. D. Aslam, C. A. Bolme, D. S. Montgomery, and K. J. Ramos. Modeling of an advanced wedge test. In *AIP Conference Proceedings*, volume 2272, 2020. URL https://doi.org/10.1063/12.0001036.